

Estimating Effect of Total Specific Atmospheric Attenuation on Performance of FSO Communication Link in South Africa

Solly P. Maswikaneng¹, Samuel O. Adebusola², Pius A. Owolawi², and Sunday O. Ojo³

¹Department of Information Technology, Tshwane University of Technology, South Africa

²Department of Computer Systems Engineering, Tshwane University of Technology, South Africa

³Department of Information Technology, Durban University of Technology, South Africa

Email: maswikanengps@tut.ac.za; adebusolaso@tut.ac.za.; owolawipa@tut.ac.za; prof.sunday.ojo@afrikt.institute

Abstract—In comparison with Radio Frequency (RF), the Free Space Optical Communication (FSOC) provides higher bandwidth, free license operation, and less initial expenditure. However, its susceptibility to changes in atmospheric weather conditions. In this paper, the impact of irradiance fluctuation on FSO systems was estimated using Rytov theory for major cities in South Africa. The extent to which the refractive index structure parameter, propagation distance and link margin affect the optical signal power at the receiver is discussed and the different methods used in evaluating the atmospheric turbulence effect are investigated. In order to achieve the stated aim, meteorological data, altitude, visibility, and wind speed were obtained from the archive of South Africa Weather Services for a period of 3years (2016-2018) over seven locations which include Cape Town, Pretoria, Upington, Bloemfontein, Emalahleni, Polokwane, East London. Results show that Emalahleni was found to possess the poor visibility of 4.4 km because of foggy conditions due to the activities of miners and other environmental factors, followed by East London with average visibility of 4.8 km. From the analysis of link margin, it was shown that FSO link attenuation reduces at higher wavelengths and long link distances due to the effect of geometric and atmospheric losses. The results show that the rate of decrease in link margin is much higher in the inland regions as compared to the coastal regions; therefore, FSO systems are prone to outage during high rainfall and longer range of connections.

Index Terms—Attenuation coefficient, Free Space Optical Communication (FSOC), Mie scattering, optical wavelength, optical wireless communication, power link margin

I. INTRODUCTION

Over the past years, communication technology and related innovations have taken a huge leap in transforming the meaning of connectivity. Nowadays, there are various communication technologies such as smartwatches, smartphones and smart T.V., etc., all of which need continuous data connectivity for an improved and better-off user experience. In [1]-[3], it was stated that with the exponential growth of data demand and an anticipated similar aggressive trend, soon it is believed that existing Radiofrequency (RF) infrastructure will face an acute spectrum shortage in coping with the exponential increase

in user data demands. There is a need for telecommunication technology that can achieve superior information rate need with unflinching quality of service at a low-level rate as conceivable, and also deliver a guaranteed linkage to the consumers. Free Space Optics (FSO) is considered the better alternative technology to meet these needs [4]. FSO is a communication system where free space act as the medium between transceivers that are line -of- sight (LOS) for successful optical signal transmission, as shown in Fig. 1. FSO offers data rates of Gigabyte per second (Gbps) and it is highly secure against eavesdropping, the use of narrow beam to transmit data from transmitter to receiver. It also uses license – free operation, has no electromagnetic interference, incurs minimal data cost, and has quick installation.

FSO is a wireless technology that uses the technology of LOS to convey a moderated ray of observable glow via the environment to deliver robust bandwidth optical links [5]. As reported by [6], it is a supplementary and/or complementary technology to the RF transmission technique. FSO technique has previously been imagined supporting meaningfully towards the unified, comprehensive, and well-off cyberspace admittance transfer of one hundred megabytes per second (100 Mbps) on behalf of each inhabitant and one gigabyte per second (Gbps) on behalf of each educational, governmental and health facility in South Africa by the year 2030. FSO has created captivating usage in entrée links (last mile solution), broadband access to remote areas, inter-building connections (point to point or multipoint), inter-satellite communication, disaster recovery, backhaul for cellular systems short-term installation for certain events, and airborne [5], [7].

Notwithstanding, with these numerous merits, the accessibility of FSO remains the major problem because it uses the propagation of light is affected by different climatic conditions, resulting in attenuation of the transmitted signal [5]. FSO uses free space channels as an interface to establish a connection between the transmitter and the receiver, as shown in Fig. 1. Therefore, the meteorological conditions must be checked before the actual execution of the FSO linkage [5].

The aim of this paper is to report on the feasibility of deploying Free Space Optical Communication (FSOC) technology by estimating the significance of the total atmospheric attenuation effects on the performance of FSO link setup in South Africa.

The rest of this paper is structured as follows: In Section II the literature review provides the various semi-empirical models for rain, fog, snow attenuation and scintillation, Section III provides a mathematical models used by Free Space Optical Communication Link (FSCOCL) to calculate the effects of atmospheric attenuation, Section IV presents and discusses the results, followed by the conclusion in Section V.

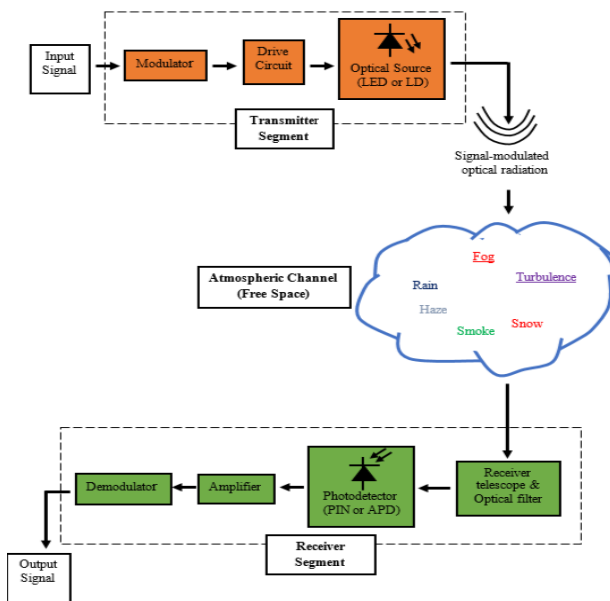


Fig. 1. Free space optical communication system [8]

The suspended particles which are present in the air because of several atmospheric weather conditions like haze, fog and rain and are normally related to the electromagnetic radiation wavelength that led to optical wave scattering [5], [8], [9]. Attenuation occurs as a result of the optical signal scattering, thus diminishes the general accessibility of the FSO system. The crucial reasons that influence the FSO link are, scintillation, scattering, and absorption [5]. Authors [10] indicated that in addition to the climate impact, the scintillation because of atmospheric turbulence influences the FSO channel. While authors [11] indicate that to counteract the scintillation, diverse strategies consisting of different schemes should be applied. However, fog is the main issue in an earthly FSO linkages, because it prompts excessive attenuation over a huge amount of time [11].

In this study, the estimation of atmospheric attenuation effects on FSO communication link in South Africa (SA) is done using the Kruse model, with several related simulation results. Based on the study done by [6], [12] SA is categorized by intense precipitation slopes impacted by the extra-tropical cloud band systems from Southern Africa. Its complex landscape and semitropical region produce good-sized spatial diversity with inside the

seasonality and amount of precipitation. Its sub-tropical location and complex topography generate significant spatial heterogeneity in the seasonality and quantity of precipitation. A study in [6] indicated that even though South Africa has severe precipitation slopes, it is mostly a semi-arid nation along with a comparatively clear atmosphere for a greater portion of the year, especially in the North-Western and Northern-Cape zones border on Namibia and Botswana [13]. All the situations presented offers greatest possibility for FSO implementation.

II. LITERATURE REVIEW

There have been various semi-empirical models for fog, rain, snow attenuations and scintillation anticipated in literatures. Statistical fog models have been proposed by authors [14], which results in improved knowledge of continental fog attenuation. While the International Telecommunications Union (ITU) delivered the guidelines aimed at designing the earthly FSO links [15], [16], in which fog attenuation coefficient is calculated simply by the visibility — which is practically defined as the distance at which bright diminutions is 2% of the original power; while in social observation, visibility remains the distance at which it is probable to differentiate a shady object against the horizon [15]. ITU adopted the technique that permits a geo-local estimation of FSO techniques performance if the visibility is understood [11].

Using digitized maps of monthly total rainfall and monthly mean surface temperature, this prediction approach determines the rainfall rate surpassed for a desired average yearly probability of exceedance and a specific location on the Earth's surface [17]. Authors [11] indicated that neither the ITU recommendations for the fog numerical methods recommended in the literature nor FSO systems design possess comparable metrics for distribution of visibility. Even though the visibility constraint is normally obtainable in weather stations or airfields archives, used for various locations the only numerical data available is a typical number of foggy periods per year for an FSO link designer.

Literature study by [2] has expanded different concerns on the perspective of FSO link communication theory. The study details the various attenuation, such as FSO transceiver, channel coding, modulation, and fading effects of atmospheric turbulence that occur in terrestrial FSO communications. However, the study presented is only focused on the various applications and limitations of earthly FSO communications whereas, this research focused on estimating the various factors that deteriorate the performance of FSO communication links over South Africa. Likewise, Bloom *et al.* [18] extensively covers several phases of the contrive of FSO links. Their research work addresses the key factors affecting the implementation of earthly FSO-link including atmospheric reduction, scintillation, orientation or movement of buildings, lunar intervention, and LOS barriers. The study also provides link budget features for satellite dish and

official receiver designs, sunbeam transmission models and handy FSO links.

Alkoholidi and Altowij investigated the impacts of rainfall meteorological conditions in Yemen on the implementation of FSO systems [19]. Precipitation as well as related weather information from various locations such as Sana, Aden and Taiz were collected by the 2008 Public Institution for Water Resources (PAWR). The rainfall rate of Taiz is the highest contrasted to Sana and Aden. In addition to rainfall weather conditions, the atmospheric diminution was explored in relation to rainfall, and it was concluded that a decrease in attenuation leads to an increase in the rainfall radius. Haider et al conducted a study on the effect of rainfall on the viability of the FSOC link over Bangladesh, considering seven cities: Dhaka, Rajshahi, Chittagong, Sylhet, Rangpur, Mymensingh and Barisal [20]. From January 2013 to June 2016, rainfall intensity was gathered from weather data for all regions of the Bangladesh Meteorological Department. It was discovered Chittagong and Sylhet obtained average precipitation compared to Rajshahi, Rangpur, Dhaka and Mymensingh, while Barisal was found to have less precipitation throughout the year. It was concluded that the rainy weather conditions have significant effects on Bangladesh's FSOC links, therefore due to the variation of atmospheric weather conditions around the world, the results obtained are from Tropical region and this cannot be used as the benchmark to design the FSO links in South Africa which is in subtropical region. Hence, there is a need to study the effects of total FSO specific atmospheric attenuation on the performance of FSOC link over South Africa. Rouissat *et al.*, 2012; conducted a study on Algeria to examine issues linked to the utilization of FSOC links regarding the effect of meteorological conditions on the implementation of FSOC links [21]. This study collected and investigated precipitation intensity information for the four cities of Algeria, Algiers, Annaba, Oran and Gardaya, to determine the effects of precipitation for FSO links. It is concluded that rainfall in Algeria will decrease from east to west and from north to south. Moreover, the utmost precipitation happens in November, December, and January in Algeria. Therefore, significant precipitation in northern Algeria remains the main challenge for FSO communication linkages.

The author [22] provides a detailed validation of the implementation of FSO communication techniques in many parts of Brazil. Firstly, a statistical pattern built on the notion of energy stability was developed towards determining the loss of FSO links. The software program was built with the developed numeric model, and this software was used to determine the power margin (dB) towards accommodating the atmospheric loss and an equivalent least visibility (km) in a function with a range of links. To check the availability of the FSOC system, visibility data from various airports in Brazil was used. The authors concluded that atmospheric attenuation was a major contributor to the availability of FSOC technology. As the clear skies of northeast Brazil are repeating, the

authors say, FSOC technology can provide the speed, quality, and consistency of optical communication at an extremely minimal cost. Their results also show that availability of more than 99% can be achieved over distances of 5 to 8 km. In other cities, such as in the South-eastern and Mid-western zones of Brazil, the FSOC system could be a feasible alternative for linkages with stretches up to 3.5 km then, availability of roughly 98%. In southern Brazil, the FSOC system can merely remain used to create exceptionally small links and intermediate or emergency links.

Analogous viability analysis for the deployment of FSOC technology in Turkey was recommended by the authors [23]. This study provides an energy cost assessment of atmospheric channels such as dispersion, assimilation, drizzle, etc., and a famous mathematical model of the simulated FSOC link was developed based on atmospheric channel theory. A simulator was utilized to investigate the availability of links that are affected by various weather conditions. The meteorological data from three airports in various cities for 2010 were obtained from three airports. The parameters used in the calculations were provided from a commercial FSOC system. In [6], the authors concluded that in the case of short-distance links, it is shown that link availability performance of 99% or more is shown in all cities. This is sufficient for enterprise networks. In Ankara, the FSOC link is fully usable even if there is a range where fog is present. The decline in precipitation typically noticed in Istanbul and Izmir remains not large enough towards affecting the accessibility of the aggregate links in that range. Also, constant losses, such as geometric and system losses, lead to the overall attenuation at the 1km link. Precipitation attenuation on long-distance links was also found to be problematic. Izmir has attained over 99% link accessibility over long-distance links.

Handura *et al.*, 2016; conducted a survey to regulate the viability of the Namibian FSOC. In this investigation, the low annual precipitation in Namibian clear skies shows the enormous ability for implementing FSOC techniques [24]. The findings of the investigation are founded on a hypothetical study. Based on long-term atmospheric data of mean visibility, wind speed, and altitude [6]. Weather measurements for 5 years from six locations (Windhoek, Walvis Bay, Ondangwa, Keetmanshoop, Grootfontein, Keetmanshoop and Katima Mulilo) in Namibian meteorological agency were collected and analyzed to calculate atmospheric attenuation under the worst and average situation of atmospheric attenuations.

By utilizing the correct mathematical models based on both atmospheric cases, the optical FSOC links distances for all locations were computed to evaluate the atmospheric losses alongside with the power link margin at each site. Assessment of meteorological information shows that FSOC optical link distances of up to 7.5 km can be achieved in inland locations from average conditions. Meanwhile, Grootfontein and Katimo Mulilo have average sunny weather year-round, with the lengthiest gap in

worst-case atmospheric situations at 6.9 km. Due to the high turbulence only Walvis, it has the shortest FSOC link distance of 3.22 km average conditions and 2.5 km in worst conditions. Authors in [24] concluded that the Namibian validation results meet the minimum visibility required for the FSOC deployment.

According to the literature discussed, the analysis of deploying of FSO link depends mostly on the state of the atmospheric weather. The performance of the FSOC link is location-dependent, as the countries differ in terms of being in Tropical, temperate, or subtropical region. As a result of unique distinctive weather conditions in South Africa, which are characterized by random and seasonal weather conditions, this presented the opportunity to investigate the estimation of the total specific attenuation effects on the implementation of FSO communication link over South Africa. This will assist in the deployment of an unfailling FSOC technology in South Africa.

III. RESEARCH METHODS

This section provides a mathematical model (Kruse Model, Rain attenuation Model, Scintillation Model), used to obtain the effects of atmospheric attenuation of FSOC. According to [25], Scattering and turbulence are the main causes of atmospheric loss in FSOC. Atmospheric losses obtained in this study are due to Mie scattering, rain-induced attenuation, and turbulence losses. Seven locations were covered in this study are Bloemfontein, Polokwane, East London, Emalahleni, Upington and Pretoria, spread across the South African seven provinces. These are key business areas with great potential for FSOC deployments. South African Weather Services (SAWS) provided meteorological data for these locations. For the determination of scattering and turbulences losses, altitude data, three years (2016-2018) wind speed and visibility for these locations were obtained from SAWS. Therefore, methods for measuring the attenuations are presented in the rest of this section.

A. Atmospheric Attenuation

This attenuation is a process in which the flux density of a parallel beam of energy decreases with increasing distance from the source as a result of absorption or scattering by the atmosphere. The atmospheric attenuation as a result of scattering [25], is mathematically given by:

$$A_{atm} = \alpha_{10}(\lambda) * L, \quad (1)$$

where $\alpha_{10}(V)$ is total-extinction and L represents the distance between the transmitter and receiver in kilometers. Also, the total extinction is further provided by:

$$\alpha_{10}(\lambda) = \sigma_m(\lambda) + \sigma_a(\lambda) + \beta_m(\lambda) + \beta_a(\lambda), \quad (2)$$

where σ_m is molecular absorption coefficient, σ_a is absorption coefficient, β_m is Rayleigh scattering coefficient and β_a is a Mie scattering coefficient. However, authors in [26] stated that FSOC wavelengths of interest make the gas absorption, aerosol absorption and molecular

scattering insignificant. Therefore, the attenuation as a result of Mie scattering is interrelated with optical signal wavelength and visibility is given by [24]:

$$\alpha_{10}(\lambda) = \beta_a = \frac{3.91}{V} * \left(\frac{\lambda}{550 \text{ nm}}\right)^{-q} \quad (3)$$

where V represent visibility (km), λ is the optical signal wavelength (nm) and q denotes a coefficient dependent on the size distribution of the scattering particles [27], in Kruse model it can be expressed as:

$$q = \begin{cases} 1.6 \text{ for } v > 50 \text{ km,} \\ 1.3 \text{ for } 6 \text{ km} < v < 50 \text{ km,} \\ 0.585 * v^{\frac{1}{3}} \text{ } v < 6 \text{ km} \end{cases} \quad (4)$$

B. Rain-induced Attenuation

Rain in R (mm/hr) is unpredictable attenuation and one of the major reasons liable to degrading the implementation of FSOC link availability and is modelled by the rain rate is given as:

$$Att_{rain} = \alpha * R^\beta \quad (5)$$

C. Scintillation Loss

Beam wander, beam spreading, and Scintillation are the three main turbulence effects [28]. Scintillation is well-defined for the temporal and spatial changes in light intensity instigated by atmospheric instability. This is the result of changes in pressure, wind, and temperature along the light propagation path, and thus the light refractive index is changing rapidly. Based on authors in [29], Scintillation is the most visible source of turbulence and Scintillation loss can be expressed as follows:

$$\sigma_{scinloss} = \left| 10 \log \left(1 - \sqrt{\sigma_{scin}^2} \right) \right| \quad (6)$$

where σ_{scin}^2 denotes scintillation index and is determine by:

$$\sigma_{scin}^2 = 2 * \sqrt{23.17 * C_2^n * L^{11/6} * \left(\frac{2\pi}{\lambda} 10^9\right)^{7/6}} \quad (7)$$

where λ represent the wavelength, C_2^n is refractive index structure parameter (RISP) ($m^{-2/3}$) and L is the link length in meters. As the refractive index of this study is location based, it is determined by using Hufnagel-Valley equation as

$$C_n^2(h) = 0.00594 * \left(\frac{w}{27}\right)^2 * ((10^{-5}h)^{10}) \exp\left(\frac{-h}{100}\right) + 2.7 * 10^{-16} \exp\left(\frac{-h}{1500}\right) + B_0 \exp\left(\frac{-h}{100}\right) \quad (8)$$

where w represents the wind speed of the wind in meters per second, h is the altitude (m) and B_0 at the ground level it represents the strength of the turbulence, given by $1.7 * 10^{-14}$.

D. Link Availability and Optical Link Margin

The authors in [30] pointed out that for unfailling FSO communication, one important task of a reliable

communication system designer is to perform the link power budget analysis. Optical maser power, glow divergence, receiver's sensitivity, coupling loss and proper selection of receiver's lens area can be defined for the FSOC to alleviate the impacts of the atmosphere. Laser power, beam divergence, receiver sensitivity, coupling loss and proper selection of receiver lens area define how the FSOC can mitigate the effects of the atmosphere.

The loss sources considered in this study are the specific attenuation due to fog, rain, and atmospheric turbulence. Thus, the link margin is the difference in the minimum received power that is expected to be the receiver's sensitivity Optical link margin is the available power beyond the receiver's sensitivity [30], defined as

$$M_{link} = P_e - S_r - A_{geo} - A_{atm} - A_{sys} \quad (9)$$

M_{link} is the link margin, P_e is the emission signal power (dBm), S_r is the sensitivity of the receiver (dBm), A_{geo} is geometric attenuation link (dB), A_{atm} atmospheric attenuation (Scintillation molecular absorption and particle scattering (dB), A_{sys} , is the interior loss of FSO equipment, in an ideal case it is always 0 dB).

In decibel the geometric attenuation is calculated by:

$$A_{geo} = -20 \log \left[\frac{dr}{(d_t + \theta L_d)} \right] \quad (10)$$

where d_t and d_r transmitter and receiver apertures diameter (cm) correspondingly, θ represent divergence beam angle (mrad) and L_d denotes link distance (km) of FSO. In research, the adopted parameters used for commercial optical transceivers were the TereScope 5000, as shown in Table I below:

TABLE I: TECHNICAL SPECIFICATIONS OF TERESCOPE 5000 [30]. DEVICE PARAMETER S

Wavelengths		650, 850 and 1550 nm
Transmitter	Output Power	95 mW
	Beam Divergence angle	2 mrad
	Transmitter Aperture diameter	3 cm
	Detector	APD
Receiver	FOV	2 mrad
	Sensitivity	-46
	Receiver Aperture Diameter	10 cm

Based on Subtropical nature of South African weather, two scenarios were adapted such as geometric loss and fog-induced loss and geometric loss and rain-induced attenuation.

Case 1: only geometric loss and fog-induced loss is represented as:

$$M_{link_{Geo\&fog}}(dB) = P_e + |S_r| - At_{geo} - At_{fog} \quad (11)$$

where

$$A_{fog} = 10 \log \left(\frac{1}{\tau(\lambda, d)} \right) \quad (12)$$

where $\tau(\lambda, d)$ denotes transmitter transmittance at the distance d . By putting equation (10) and equation (12) into equation (11) it resulted in:

$$M_{link_{Geo\&fog}}(dB) = P_e + |S_r| - 20 \log \left[\frac{dr}{(dt + \theta L_d)} \right] - 10 \log \left(\frac{1}{\tau(\lambda, d)} \right) \quad (13)$$

In this study, the fog attenuation was calculated at three optical wavelengths of 650, 850, 1550 nm while link distances of 1,2,3, ...,10 km and 2% threshold transmittance at location based average visibility over the selected locations in South Africa.

Case 2: Consider geometric attenuation and rain-induced loss is represented as:

$$M_{link_{Geo\&Rain}}(dB) = P_e + |S_r| - At_{geo} - At_{rain} \quad (14)$$

where

$$At_{rain} = (0.3988 * R^{0.7601}) * L_d \quad (15)$$

substituting (10) and (15) into equation (14) it resulted into:

$$M_{link_{Geo\&Rain}}(dB) = P_e + |S_r| - 20 \log \left[\frac{dr}{(dt + \theta L_d)} \right] - (0.3988 * R^{0.7601}) * L_d \quad (16)$$

where all previous parameters definitions are taken. Average Rain rate values are used to compute the rain-induced loss. The values are used to cover the various types of precipitation observed in these study locations and same link distances are used in the calculations.

Case 3: Consider geometric attenuation and Scintillation loss, its link margin can be expressed as:

$$M_{link_{Geo\&Scint}}(dB) = P_e + |S_r| - At_{geo} - At_{scint} \quad (17)$$

Then, by substituting (6) into (17), the link margin becomes:

$$M_{link_{Geo\&Scint}}(dB) = P_e + |S_r| - 20 \log \left[\frac{dr}{(dt + \theta L_d)} \right] - \left[\left| 10 \log \left(1 - \sqrt{\sigma_{scin}^2} \right) \right| \right] \quad (18)$$

where: σ_{scin}^2 is expressed in (6). Scintillation loss was calculated based on the location-based values of C_n^2 which was used to determine the turbulence state of the locations based in South Africa. Optical wavelengths of 650, 850 and 1550 nm were utilized according to specified link distances.

The power margin of optical link indicated that the extent by which a method can recompense for dispersal and instability losses at a given range [30].

The length of an FSOC link will correctly function if $M_{link}(L_d^*) \geq At_{atm}(L_d^*)$ where $At_{atm}(L_d^*)$ represent atmospheric losses, the total of dispersal and instability losses at L_d^* . If L_d^* in kms, the required minimum visibility (Vis_{min}) for accurate FSOC operation is explained by author [28] as:

$$Vis_{min} = \frac{17L_d}{M(L_d)} \left(\frac{\lambda * 10^9}{550} \right)^{-q(vis)} \quad (km) \quad (19)$$

$$M_{link} = M_a - 20 \log L \quad [dB] \quad (20)$$

where: $M_a = 82$, all constant values in equation (8).

III. RESULTS AND DISCUSSIONS

In this study, atmospheric attenuation was calculated by accumulation of scattering, rain, and turbulence losses. In literature review it is indicated that the atmospheric attenuation is visibility dependent while turbulence loss is wind speed and altitude dependent.

A. Atmospheric Attenuation

Average visibility was calculated based on the South African locations in order to determine the average attenuation for those locations. At various average distance visibility, Mie scattering attenuation and the specific mean attenuation coefficients were calculated by using (1) and (3). In Fig. 2, the average attenuation at 650, 850 and 1550 nm optical signal wavelengths that are built upon 2% transmittance threshold over the period of three years (2016 – 2018) by utilizing Kruse model is illustrated.

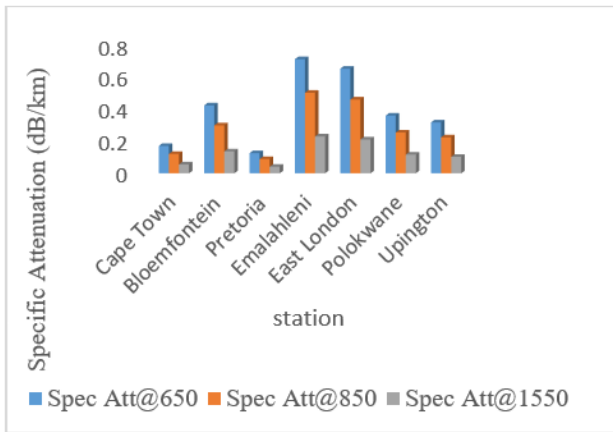


Fig. 2. Average specific attenuation at various optical signal wavelengths and 2% transmittance threshold for the period of the study.

Over the three years' period, Pretoria had the maximum average visibility through the year owing to its fine weather, with the lowest attenuation of 0.13, 0.09 and 0.04 dB/km at 650, 850 and 1550 nm optical signal wavelengths respectively. Emalaheni recorded the lowest average visibility of 4.4 km with the average attenuation of 0.72, 0.51 and 0.23 dB/km at 650, 850 and 1550 nm wavelengths correspondingly. From the values of 650 nm to that of 850 nm, the estimated attenuation declines by 29.17% while from 650 nm to 1550 nm, attenuation values decline by 68.06%. Another location that experienced foggy events in East London with an average visibility of 4.8 km and an average attenuation of 0.66, 0.46 and 0.21 dB/km at 650, 850 and 1550 nm wavelengths respectively. From 650 nm to 1550 nm, the attenuation values decline by 68.18%. Table II provides the results of the average Mie scattering coefficient determined from each selected location. From Fig. 2, and Table II, it can be observed that

the locations with the highest scattering attenuation attribute to its poorer visibility. This can be determined by comparing Emalaheni with low average visibility of 4.4 km and Pretoria with high average visibility of 24.93 km, with Pretoria displaying a low Mie scattering influence while Emalaheni recording a high attenuation for the same distances and wavelengths. Therefore, from the obtained data, we can conclude that the lengthier the mean visibility span, the smaller the attenuation coefficient, and vice versa.

TABLE II: AVERAGE VISIBILITY AND ATTENUATION COEFFICIENTS OVER THE PERIOD OF STUDY

Location	Average visibility (km)	Average attenuation coefficient (dB/km) at 650 nm	Average attenuation coefficient (dB/km) at 850 nm	Average attenuation coefficient (dB/km) at 1550 nm
Cape Town	18.370	0.171	0.121	0.055
Bloemfontein	7.4	0.425	0.300	0.137
Pretoria	24.93	0.126	0.089	0.041
Emalaheni	4.4	0.715	0.505	0.231
East London	4.8	0.656	0.463	0.212
Polokwane	8.7	0.362	0.255	0.117
Upington	9.87	0.319	0.225	0.103

B. Rain-induced Attenuation

For the determination of the attenuation as a result of the intensity of rain, the meteorological data linked to rain intensity of different locations in South Africa were obtained from SAWS over the period of three years from 2016 - 2018. The average seasonal data (Summer – December to February, Autumn – March to May, Winter – June to July and Spring September to November) was calculated. Table III provides the summary of the average seasonal precipitation over the period of the study. In Table III, it is observed that Upington and Cape Town experienced the highest average rain rate of 10.676 and 6.195 mm/hr for the period of study in Winter respectively. This may be as a result of the effect of the cyclones or cold fronts on the two locations. These results are consistent with the SAWS statement that precipitation is highest in the eastern and southern mountains, including the Drakensberg Mountains, from the Rim through Mpumalanga, Kwazulu- Natal and into the northern part of the Eastern Cape. While East London, Emalaheni, Pretoria, Polokwane and Bloemfontein experienced their rainy season in summer with an average rain rate of 7.163, 7.162, 6.376, 6.879 and 6.515 mm/hr respectively. This is because enough heat is generated at this location and warm moist air rises and settles from cooling to condensing thunderstorms.

The attenuation as a result of precipitation is determined by computing the specific attenuation constant utilizing (5) is indicated in Fig. 3.

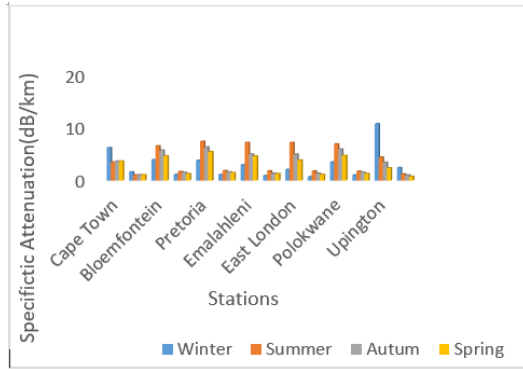


Fig. 3. Average specific precipitation attenuation over South Africa for the period of study.

It was observed that locations with high precipitation recorded higher attenuation coefficients. As a result, Uppington recorded a 2.41 dB/km maximum specific attenuation coefficient and a 0.675 dB/km minimum specific attenuation coefficient.

TABLE III: SUMMARY OF AVERAGE SEASONAL RAIN RATE AT VARIOUS LOCATIONS IN SOUTH AFRICA OVER THE PERIOD OF STUDY

Seasons	Cape Town	Bloemfontein	Pretoria	Emalahleni	East London	Uppington
Winter	6.195	3.891	3.795	2.965	2.062	3.475 10.68
Summer	3.451	6.515	6.376	7.162	7.163	6.879 4.393
Autumn	3.645	5.688	5.302	4.962	4.956	5.909 3.443
Spring	3.651	5.688	5.452	4.596	3.841	4.692 2.359

C. Atmospheric Turbulence Effect Over South Africa for the Period of Study

For calculation of RISP C_n^2 for all regions, average wind speeds (m/s) and the altitude values (m) for three years were used, by utilizing the Hufnagel-Valley model in (8). The results obtained are shown in Table IV. However, with the Hufnagel-Valley model, only the influence of altitude is dominant since wind speed does not significantly affect RISP. The scintillation index, or atmospheric instability loss, can be finalized by changing the space between two telecommunication transceivers using RISP. It is observed that the elevation of the location has a greater effect on the scintillation effect. Significantly, high scintillation indices can be obtained in low-altitude coastal regions, but significantly low scintillation indices are recorded in high-altitude inland regions. As shown in Table IV, Rustenburg, Bloemfontein, Pretoria, Polokwane and Uppington, have the lowest average wind speeds of 2.9, 3.2, 3.2, 3.4, and 3.5 m/s, respectively, while Cape Town at 5.8 m/s experienced uppermost wind speed. The highest altitude of 1635 m is recorded at Emalahleni with a scintillation index of 0.0049 (dB) and RISP of $9.08 \times 10^{-17} m^{-2/3}$ at a link distance of 1km and wavelengths of 650 nm, while Cape Town with the lowest elevation of 22 m has the highest scintillation index of 0.756 (dB) and RISP of $1.39 \times 10^{-14} m^{-2/3}$ over the same link. Therefore, due to its high heat capacity, longer heating times in coastal areas will result in a higher scintillation index than in the cool inland atmosphere.

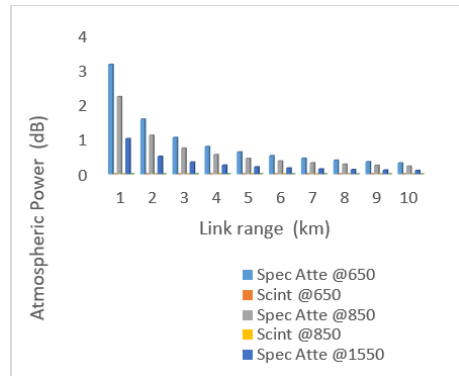
The implication of this is that in planning FSOC links in the study locations more attention should be given to coastal regions because the signal transmitted would be more attenuated compared to the inland region.

TABLE IV: RISPS, ALTITUDE, SCINTILLATION INDEX AND WIND SPEED FOR SOUTH AFRICA

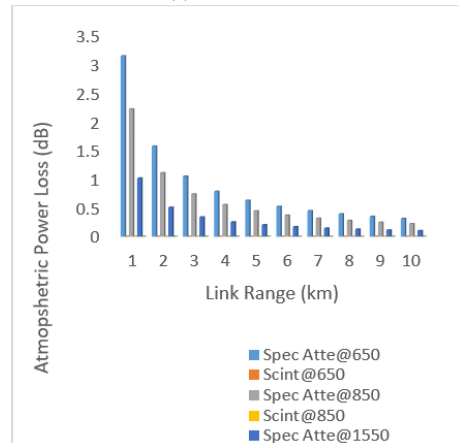
Region	Avg Wind Speed (m/s)	Altitude (m)	Scintillation Index(dB)	RISP ($m^{-2/3}$)
East London	5	35	0.672	1.22×10^{-14}
Durban	3.4	23	0.756	1.38×10^{-14}
Polokwane	3.4	1334	0.00609	1.11×10^{-16}
Pretoria	3.2	1335	0.00609	1.11×10^{-16}
Emalahleni	4	1635	0.0049	9.08×10^{-17}
Rustenburg	2.9	1162	0.0068	1.25×10^{-16}
Uppington	3.5	810	0.0089	1.63×10^{-16}
Bloemfontein	3.2	1353	0.00601	1.09×10^{-16}
Cape Town	5.8	22	0.756	1.39×10^{-14}

1) Comparison of Mie scattering and scintillation index over South Africa for period of study

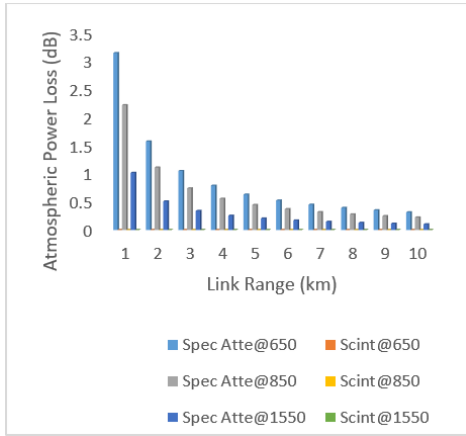
This section relates the variation of two atmospheric losses i.e. Mie scattering and scintillation loss over south Africa for the period of study. It is seen in Fig. 4(a-g), that in all the locations of study, the effect of Mie Scattering attenuation is higher than the turbulence loss at various wavelength considered in this study. The turbulence loss for each location in South Africa is negligible for the implementation of FSOC technology compared to total attenuation effect.



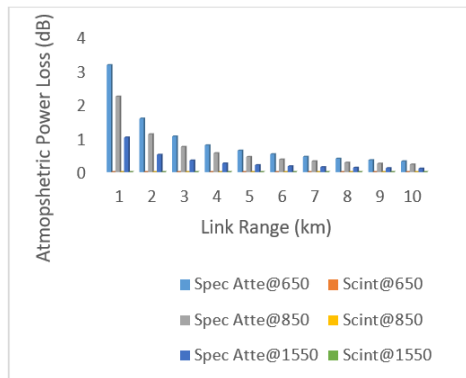
(a) East London



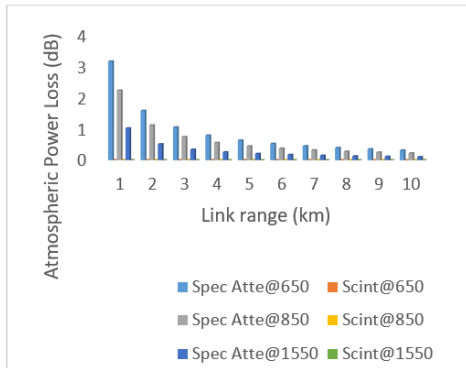
(b) Polokwane Power Loss



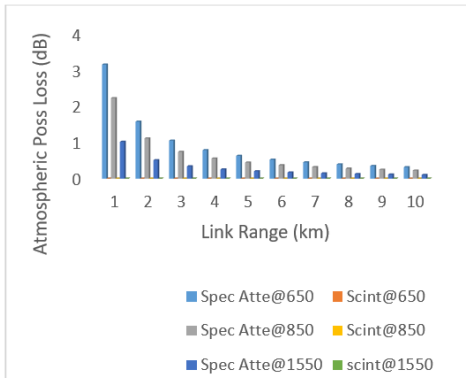
(c) Bloemfontein Power Loss



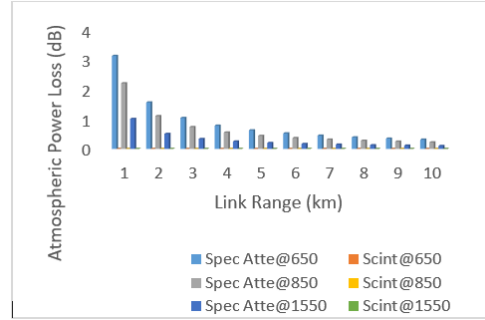
(d) Pretoria Power Loss



(e) Cape Town Power Loss



(f) Emalaheni Power Loss



(g) Upington Power Loss

Fig. 4. Variation of Mie scattering and scintillation index at various wavelengths over South Africa. (a) East London (b) Polokwane (c) Bloemfontein (d) Pretoria (e) Cape Town (f) Emalaheni (g) Upington

D. Optical Link Margin and Link Availability

Geometric loss and scattering effects

This section presents the results of link margin as a result of the combination of geometric loss effects and atmospheric Mie scattering attenuation effects over South Africa for the period of study. The result obtained was computed using (13). Fig. 5, shows the analysis of link margin using geometric loss and attenuation due to fog at various wavelengths (650 nm, 850 and 1550nm) and link distance. Considering 650 nm and a link distance of 1 km, the achievable various link margins over the studied locations, Cape Town, Bloemfontein, Pretoria, Emalaheni, East London, Polokwane, and Upington are 33.41, 34.61, 35.60, 33.16, 35.52, 34.39 and 34.86 dB respectively. Also, at 1550 nm with respect to the same link distance and locations, link margins obtained are 35.29, 35.69, 36.01, 35.22, 35.33, 35.62 and 35.77 dB respectively. It is shown from Fig. 5, that the link margin increases with the wavelength. It can also be observed in Fig. 5, that the link distances increase as the link margin decreases.

The percentage of difference in all the locations at 1 km and 10 km at 650 nm over Cape Town, Bloemfontein, Pretoria, Emalaheni, East London, Polokwane, and Upington for the period of study are 46.6, 17.7, 2.1, 54.7, 43.2, 21.8, and 13.3 % while at 1550 nm, and considering the same link distance, the percentage of decrement 6.4, 1.1, 2.9, 7.6 5.9, 9.1, 0.0024%, respectively.

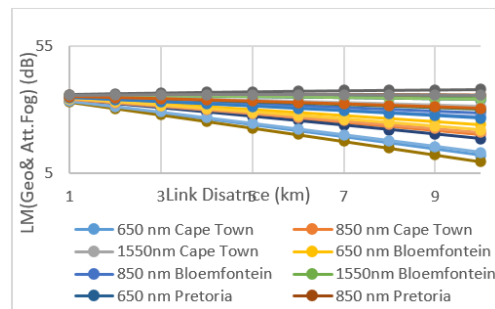


Fig. 5. Analysis of link margin using geometric loss and attenuation due to fog at various wavelengths over South Africa.

Geometric loss and rain-induced attenuation

This section presents the result of link margin as a result of effects combination of geometric loss and rain attenuation over South Africa for the period of study. The result obtained was computed using (16). Fig. 6, demonstrates the graph plotting the link margins as a result of the combined effects of rain-induced attenuation and geometric loss at various locations of the study. Link margins at 3 km are 23.82, 14.53, 13.82, 10.34, 16.35, 4.72 and 21.75 dB respectively for Cape Town, Bloemfontein, Pretoria, Emalaheni, East London Polokwane and Uppington based on the rain rate indicated in Table 5. It is shown in both Fig. 6, and Table V that as the link distance increase, the link margin decreases with disregard of rain rate. As depicted in Table V, the higher the rain rate, the lesser the link margin. Polokwane with rain rate of 77 mm/hr has Link Margin of 25.37 dB as compared to Cape Town with a rain rate of 24 mm/hr has a link margin of 31.73 dB. At a link distance 10 km, the link margin is -4.58, -35.55, -37.93, -49.53, -29.29, -68.24, and -11.47 dB across all the locations of study, the minus sign means that the link margin was unavailable at all the locations. From the link distance of 1km to 10 km at rain rate of 24 mm/hr

in Cape Town, the link margin reduces by 114.43 % whereas in Polokwane with a rain rate of 77 mm/hr the link margin reduces by 369.34 %.

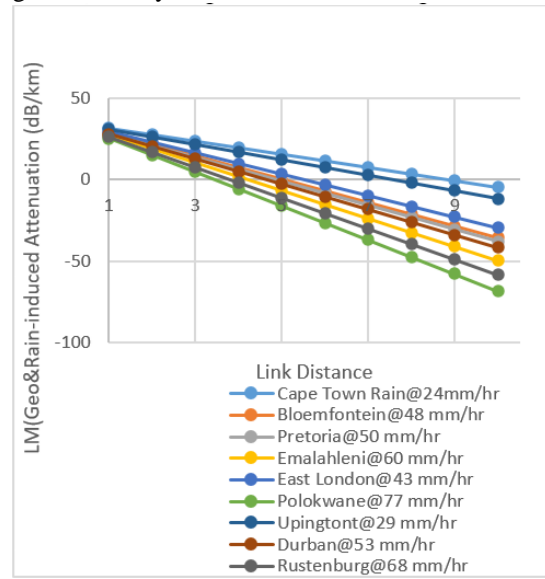


Fig. 6. Analysis of Link Margin using Geometric loss and Attenuation due to Rain rate at various wavelengths over South Africa

TABLE V: SUMMARY OF LINK MARGIN DUE TO THE EFFECT OF GEOMETRIC AND RAIN-INDUCED LOSSES

Link Range (km)	Cape Town Rain@24mm/hr	Bloemfontein@48 mm/hr	Pretoria@50 mm/hr	Emalaheni@60 mm/hr	East London@43 mm/hr	Polokwane@77 mm/hr	Uppington@29 mm/hr
1	31.73	28.64	28.39	27.24	29.24	25.37	31.04
2	27.79	21.59	21.13	18.80	22.81	15.06	26.41
3	23.83	14.53	13.82	10.34	16.35	4.72	21.75
4	19.83	7.44	6.49	1.85	9.87	-5.63	17.06
5	15.80	0.32	-0.87	-6.67	3.35	-16.00	12.35
6	11.77	-6.82	-8.25	-15.20	-3.18	-26.43	7.62
7	7.71	-13.97	-15.6	-23.76	-9.73	-36.85	2.87
8	3.63	-21.150	-23.1	-32.33	-16.3	-47.30	-1.90
9	-0.47	-28.343	-30.5	-40.92	-22.9	-57.76	-6.68
10	-4.58	-35.55	-37.9	-49.53	-29.5	-68.23	-11.48

Geometric loss and atmospheric turbulence

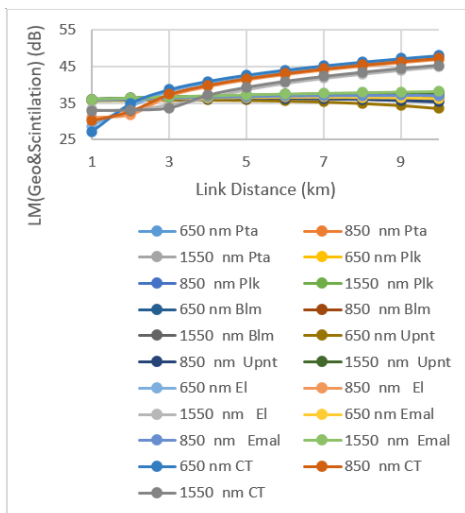


Fig. 7. Analysis of Link Margin using Geometric loss and attenuation due to turbulence at various wavelengths over South Africa.

Fig. 7, shows the curve of variation of link margin due to geometric and scintillation loss with link distance. The results obtained are computed from (18). It is shown from Fig. 5c, that the inland locations like, Pretoria, Polokwane, Bloemfontein, Uppington and Emalaheni, have their link margin increases at lower link distances and reduces at a higher link distance above 8 km while in the coastal regions like, East London and Cape Town have their link margin increases as the link distance increases across all the wavelengths. The percentage increase of the link margin over East London for link distances of 1 and 10 km at 650 nm is 65.74% and at 1550 nm is 35.2% while the percentage increase in Cape Town at 650 nm is 76.35% and at 1550 nm is 37.51%.

Link Availability

The power margin of the optical link is the extent by which a technique can recompense for dispersal and instability losses at an allotted span [28]. For a FSOC link to be accessible, the power link margin must be greater than or equal to the atmospheric loss consisting of Mie

scattering and turbulence loss of a location, hence the installation of FSOC link becomes a problem. In estimating the power link margin, (20) was used. The points in Fig. 8(a-c), where the link margin intersects with the total atmospheric loss lines indicate the points of optimum link distance for different optical signal wavelengths. At 650 nm as shown in Fig. 8a, the optimum link distance achieved across all the locations Cape Town, Pretoria, East London, Upington, Bloemfontein, Emalahleni, and Polokwane is 15.1, 45.0, 15.2, 15.3, 20.1, 15.25 and 20.2 km respectively, whereas at 850 nm as shown in Fig. 8b, the optimum link distance achieved across all the studied locations are 18.2, 19.0, 30.0, 32.0, 28.0, 18.20 and 29.2 km respectively. In the same view, at 1550 nm as shown in Fig. 8c, the optimum link distance achieved across all the locations Cape Town, Pretoria, East London, Upington, Bloemfontein, Emalahleni, and Polokwane is 35.80, 35.80, 36.0, 25.20, 30.0, 36.20 and 49.2 km respectively. In planning FSO communication systems in South Africa, it is posited that telecommunication engineers should make use of the recommended link distances for various optical signal wavelengths over South Africa for efficient deployment of FSO links. From Table VI, it is seen that the minimum visibilities are less than the required average visibilities across all the locations as shown in Table II, hence, under average conditions, the FSOC systems in all the studied locations in the country of study can be planned for the highest link distances obtained.

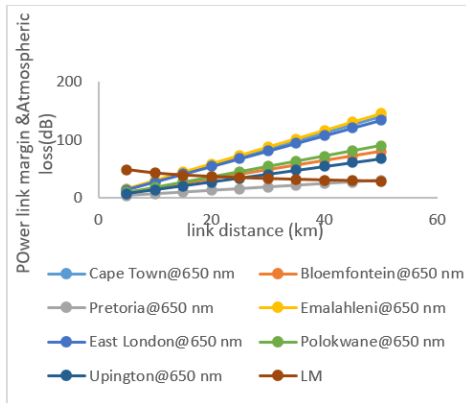


Fig. 8. (a) Link margin against Link distance at Wavelength of 650 nm

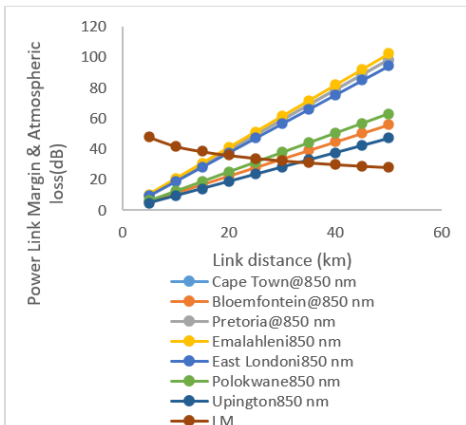


Fig. 8. (b) Link Margin against Link distance at Wavelength of 850 nm

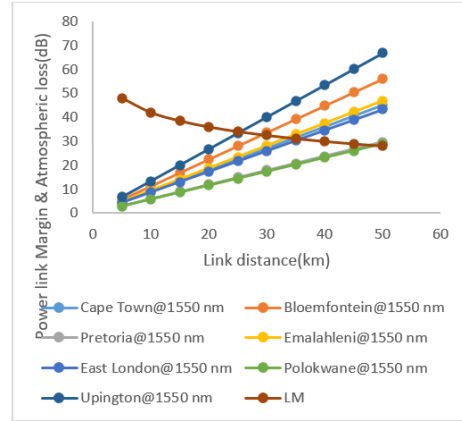


Fig. 8. (c) Link margin against Link distance at 1550 nm

TABLE VI: LINK AVAILABILITY AT 1550 NM

locations	Min visibility (km)
Cape Town	0.9451
Bloemfontein	0.3818
Pretoria	1.2856
Emalahleni	0.2270
East London	0.2476
Polokoane	0.4489
Upington	0.5092

V. CONCLUSION AND FUTURE WORK

This study investigated specific attenuation and scintillation of earthy FSOCs in South Africa due to fog and rain. Seven locations, namely Polokwane, Pretoria, Bloemfontein, Emalahleni, East London, Cape Town and Upington were selected across the country as they are fair representations of varying weather conditions in South Africa. Retrieved three years (2016 – 2018) average visibility and rain data were utilized to calculate rain- and fog-induced losses at various optical wavelengths of 650, 850 and 1550 nm and two percent transmittance thresholds. Wind speed and Altitude for all locations were retrieved. For the computation of atmospheric attenuation, Mie scattering for the locations of the study average visibility data was utilized. Emalahleni was found to possess the lowest visibility of 4.4 km because of foggy conditions due to the mines and other environmental factors, followed by East London with average visibility of 4.8 km. From the results obtained, it was found that the non-attenuation due to fog generally decreases as the optical wavelength increases. The minimum visibility required for all locations is below average, therefore, it can be concluded that FSOC is a feasible technique under average atmospheric conditions.

It was also observed that Upington and Cape Town experienced the highest average rain of 10.676 and 6.197 mm/hr respectively for the period of study in winter, this is due to the effects of cyclones or cold fronts. East London, Emalahleni, Pretoria, Polokwane and Bloemfontein experience their rainy season in summer with an average rain rate of 7.163, 7.162, 6.376, 6.879 and 6.515 mm/hr respectively, this is due to the heat that is generated at these locations, warm moist air, and cooling to condensing

thunderstorm. Also, the locations with high precipitation recorded higher attenuation coefficient. Turbulence equations obtained from the literature were used to calculate the turbulence losses of all over the locations of study. Significantly high scintillation indices can be obtained in low-altitude coastal regions, but significantly low scintillation indices are recorded in high-altitude inland regions. The implication of this is that in planning FSOC links in the study locations, more attention should be given to coastal regions because the signal transmitted would more be attenuated compared to the inland region.

The results obtained by link margin analysis due to geometric and fog loss were found to reduce FSO link attenuation at higher optical wavelengths. It also shows that the adoption of higher operating wavelengths is effective for reducing attenuation, depending on the link range. While considering the geometric and fog-induced losses results at 3km, similar trends were observed based on the FSO system design being used in all the locations where the rainfall rate of the study was considered. The results show that the rate of decrease in link margin is much higher, therefore, FSO systems are prone to disconnection at high rainfall and a longer range of connections.

Conclusively, the results observed in this study are that FSOC is a promising technology in South Africa. In planning FSO communication systems in South Africa, the telecommunication engineers are hereby advised to consider using the recommended link distances for various optical signal wavelengths over South Africa for efficient deployment of FSO links. Regarding the future work of this research, the proposed study was based on the theoretical model, the practical deployment of this research should be done as a part of future work. Results of practical deployment and theoretical results should be compared.

CONFLICT OF INTEREST

All authors declare no conflict of interest

AUTHOR CONTRIBUTIONS

Maswikaneng PS and Adebusola S.O contacted the research and wrote the paper

Owolawi P.A and Ojo SO analysed the data.

All authors approved the final version of the journal

ACKNOWLEDGMENT

The Authors would like to express our gratitude to South African Weather Services for providing weather data for the study.

REFERENCES

[1] S. Chauhan, R. Miglani, L. Kansal, S. Gaba, and M. Masud, "Performance analysis and enhancement of free space optical links for developing state-of-the-art smart city framework," *Photonics*, vol. 7, no. 4, pp. 132-148, Dec. 2020.

[2] M. A. Khalighi and M. Uysal, "Survey on free space optical communication: A communication theory perspective," *IEEE Comm. Surv. Tutor.* vol. 16, no. 4, pp. 2231-2258, Dec. 2014.

[3] Z. Ghassemlooy, W. Popoola, and S. Rajbhandari, *Optical Wireless Communications: System and Channel Modelling with Matlab*, 1st ed. CRC Press: Boca Raton, FL, USA, 2019, Ch. 1, pp. 1-34.

[4] P. S. Maswikaneng, P. A. Owolawi, S. O. Ojo, Z. Mahlobogwane, and M. I. Mphahlele, "Climatic effects on free space optics link: South African Climate," in *Proc. International Conference on Intelligent and Innovative Computing Applications (ICONIC)*, vol. no. pp.1-5 Dec. 2018.

[5] Basehel, R. Islam, M. Habaebi, and S. Ahmad, "Availability prediction methods for terrestrial free-space-optical link under tropical climate," *Indonesian Journal of Electrical Engineering and Computer Science*, vol. 10, no. 1, pp. 224-229, April 2018.

[6] J. Mohale, M. R. Handura, T. O. Olwal, and C. N. Nyirenda, "Feasibility study of free-space optical communication for South Africa," *Optical Engineering*, vol. 55, no. 5, 2016.

[7] Basel and R. Islam, "Availability assessment of free-space-optics link with rain data from tropical climates," *Journal of Lightwave*, vol. 35, no. 19, pp. 4282-4288, April 2017.

[8] A. A. Basahel, I. Rafiqul, M. H. Habaebi, and S. A. Zabidi, "Availability modeling of terrestrial free-space optical links using fade statistics from tropical climate," in *Proc. IEEE International Conference on Smart Instrumentation, Measurement and Applications (ICSIMA)*, Putrajaya, Malaysia, vol. 158, April 2018, pp. 105-111.

[9] F. Nadeem, V. Kvicera, M. S. Awan, E. Leitgeb, S. S. Muhammad, and G. Kandus, "Weather effects on hybrid FSO/RF communication link," *IEEE Journal. Sel. Areas in Communication*, vol. 27, no. 9, pp. 1687-1697, Dec. 2009.

[10] Quwaiee, H. C. Yang, and M. S. Alouini, "On the asymptotic capacity of dual-aperture FSO systems with generalized pointing error model," *IEEE Transactions on Wireless Communications*, vol. 15, no. 9, pp. 6502-6512, Sept. 2016.

[11] Sousa, M. P. Queluz, and A. Rodrigues, "An efficient visibility prediction framework for free-space optical systems," *Wireless Pers Communication*, vol. 96, pp. 3483-3498, April 2017

[12] N. C. G. Hart, C. J. C. Reason, and N. Fauchereau, "Cloud bands over Southern Africa: Seasonality, contribution to precipitation variability and modulation by the MJO," *Springler-Verlag Berlin Heidelberg*, Germany, vol. 41, pp. 5-6, Sept. 2013.

[13] Saexplorer.co.za. Map of South Africa. (2015). [Online]. Available: <http://www.saeplorer.co.za/southafrica/map/southafricamap.asp>

[14] M. S. Khan, M. S. Awan, S. S. Muhammad, M. Faisal, F. Nadeem, and E. Leitgeb, "Probabilistic model for free-space optical links under continental fog conditions," *Radioengineering*, vol. 19, no. 3, pp. 460-465, Sept. 2010.

- [15] ITU. Prediction Methods Required for the Design of Terrestrial Free-space Optical Links, Recommendation ITU-R P.1814, 2007.
- [16] ITU. Propagation Data Required for the Design of Terrestrial Free-space Optical Links, Recommendation ITU-R P.1817, 2012.
- [17] ITU. Characteristics of Precipitation for Propagation Modelling, Recommendation ITU-R P.837, 2012.
- [18] S. Bloom, E. Korevaar, J. Schuster, and H. Willebrand, "Understanding the performance of free-space optics," *J. Opt. Netw. (OSA)*, vol. 2, no. 6, pp. 178–200, June 2003.
- [19] K. Shahiduzzama, M. F. Haider, and B. K. Karmaker, "Terrestrial free space optical communications in bangladesh: Transmission channel characterization," *International Journal of Electrical and Computer Engineering*, vol. 9, pp. 3130–3138, Dec. 2019.
- [20] M. Rouissat, A. R. Borsali, and M. E. Chikh-Bled, "Free space optical channel characterization and modeling with focus on algeria weather conditions," *International Journal of Computer Network and Information Security*, vol. 4, no. 3, pp. 17–23, April 2012.
- [21] J. R. Souza and P. B. Harboe, "Free space optical communication systems: feasibility study for deployment in Brazil," *Journal of Microwaves Optoelectronics*, vol. 3, no. 4, pp. 58-66, May 2004.
- [22] K. Ozturk, "Simulation of free space optical links under different atmospheric conditions," M.S. thesis, school of Natural and Applied Sciences, Cankaya University, Turkey, 2011.
- [23] M. R. Handura, K. M. Ndjaver, C. N. Nyirenda, and T. O. Olwal, "Determining the feasibility of free space optical space communication in Namibia," *Opt. Comm.*, vol. 366, pp. 425-430, May 2016.
- [24] A. K. Prokes, "Atmospheric effects on availability of free space optics systems," *Opt. Eng.*, vol. 48, no. 6, June 2009.
- [25] K. Altowij and A. Alkholodi, "Effect of clear atmospheric turbulence on quality of free space optical communications in Western Asia," *Space Optical Communications in Western Asia. INTECH Open Access Publisher*, Ch. 2, pp. 41-74, March 2012.
- [26] S. M. Rajendrakumar and M. Karrypaswamy, "Analysis of link availability in FSO-OFDM system under various climatic conditions," *Engineering Journal*, vol. 19, no. 1, pp. 85-95, Jan. 2015.
- [27] K. Tsumakato, A. Hashimoto, Y. Aburukwa, and M. Matsumoto, "The case for free space," *IEEE Microwave Magazine*, vol. 10, July 2009.
- [28] M. O. Ajewole, P. A. Owolawi, J. S. Ojo, and R. M. Adetunji, "Fog and rain attenuation characterization and performance of terrestrial free space optical communication in Akure, Nigeria," *APTİKOM Journal on computer Science and Information Technologies*, vol. 4, no. 3, pp. 125-134, Oct. 2019.
- [29] ITU-R, Fixed Service Applications Using Free-space Optical Links, Report ITU-R F. 2106, April 2010.
- [30] E. Korevaar, *et al.*, "Understanding the performance of free optics," *J. Opt. Networking*, vol. 2, no. 6, pp. 178-200, June 2003.

Copyright © 2022 by the authors. This is an open access article distributed under the Creative Commons Attribution License ([CC BY-NC-ND 4.0](https://creativecommons.org/licenses/by-nc-nd/4.0/)), which permits use, distribution and reproduction in any medium, provided that the article is properly cited, the use is non-commercial and no modifications or adaptations are made.

Solly P. Maswikaneng received the B-Tech in Information Technology from Pretoria Technikon in 2008 and the M-Tech in Communication Networks, Tshwane University of Technology in 2011; both in South Africa. He is currently pursuing the Ph.D. degree with Department of Information Technology (Communication Networks), Tshwane University of Technology, Pretoria, South Africa. His research interests include are signal processing in wireless and mobile communication networks, Free Space Optics, IoT, Security and privacy in wireless and wired networks, Cloud computing and Artificial Intelligence.

Samuel O. Adebisola received the BSc. Honours from the University of Ado Ekiti, Nigeria in 2010 and MTech. from the Federal University of Technology, Akure, Nigeria (FUTA), in 2016, both in Physics. He is currently pursuing the Ph.D. degree with the Department of Computer Systems Engineering, Tshwane University of Technology, Pretoria, South Africa. His research interests include satellite communication, free space optics, wireless and mobile communication networks, cloud computing, Artificial intelligence and machine learning, deep learning, and data engineering.

Pius A. Owolawi received BTech. in Physics with electronics in 2001 from the Federal University of Technology, Akure, Nigeria (FUTA), M.Sc. and Ph.D. degrees in electronic engineering from University of KwaZulu-Natal, South Africa, in 2006 and 2010, respectively, and the Ph.D. He is currently a professor of Electronics Engineering. Since 2017, he has been with Tshwane University of Technology, Pretoria, South Africa as the head of the Department of Computer Systems Engineering. His current research interests include, Internet of things, Artificial intelligence, deep learning, data engineering, machine learning, robotics engineering and Control systems.

Sunday O. Ojo received Ph.D. in Computing science from Glasgow in 1984. He is currently a Professor of Computer Science. He has over 40 years of career as an academic in several African Universities. He held positions as a Research & Innovation Professor, Head of Department, and faculty Executive Dean. He has successfully promoted several Doctoral and master's students and currently promotes the same at Tshwane University of Technology and Durban University of Technology, South Africa.